PCCP

PAPER

Check for updates

Cite this: *Phys. Chem. Chem. Phys.*, 2017, **19**, 18481

Molecular studies of Cs adsorption sites in inorganic layered materials: the influence of solution concentration

Kiminori Sato *[a] and Michael Hunger[b]

Received 30th April 2017,
Accepted 28th June 2017

DOI: 10.1039/c7cp02814h

rsc.li/pccp

Radioactive Cs released into a soil environment migrates along with groundwater in a manner dependent on Cs concentration. Data on the variation of Cs adsorption as a function of solution concentration are an essential prerequisite to successful decontamination work in Fukushima. To aid the ongoing decontamination work, the adsorption of Cs in aqueous solution across a wide Cs^+ molarity range is studied for the case of saponite clay as adsorbent, an inorganic layered material that is an abundant mineral in the soil environment. The local molecular structures, *i.e.* nanosheet surfaces, nanosheet edges, and oncoming hexagonal cavities, participating in Cs adsorption are qualitatively highlighted by means of a recently developed analytical method using data from a conventional elution test, ^{133}Cs magic-angle-spinning nuclear magnetic resonance (MAS NMR), and the radiocesium interception potential (RIP) [K. Sato, *et al.*, *J. Phys. Chem. C*, 2016, **120**, 1270]. The concentrations of nanosheet edges amount to between 100 and 400 mmol kg^{-1}, which are not substantially different from those of the nanosheet surfaces, generally regarded as the main decontamination sites. This unambiguously implies that the nanosheet edges should be targeted as the molecular sites for decontaminating radioactive Cs, in addition to the nanosheet surfaces.

Introduction

Following the nuclear crisis at Fukushima, legislation for a range of special measures has come into force. Consequently, a huge effect has been dedicated to the decontamination of sites affected by radioactive Cs, particularly in the special decontamination area, *i.e.* the 11 municipalities in the restricted zone and the planned evacuation zone.[1] According to an announcement on 'Progress in the Special Decontamination Area' from Japan's Ministry of the Environment, the decontamination work has effectively reduced dose levels in the special decontamination area.[2] For example, a high reduction rate exceeding 80% has been achieved in a children's playground in the area, which has been acknowledged as evidence of the effectiveness of the decontamination work. According to government-formulated decontamination guidelines, as much as 5 cm of the soil surface should be scraped away to obtain adequate results, yielding a large amount of contaminated soil.[3] The total volume of contaminated soil discharged through the decontamination work has been estimated to reach 16–22 million m^3 in the Fukushima prefecture.[4] The urgency of reducing the volume of contaminated soil has become a serious concern with respect to the acceleration of ongoing work as well as decreasing the cost of decontamination.[5]

The contaminated soil is reduced in volume through water treatment, using water circulation equipment specially designed for the soil resultant from the Fukushima crisis.[6] The fundamental principle of volume reduction is that radioactive Cs dissolved in water tends to strongly adsorb onto the surface of two-dimensional (2D) nanosheets, a basic structural unit of clay minerals. Smaller particles of contaminated soil exhibit higher specific surface area for Cs adsorption in aqueous solution, enabling them to associate with a larger amount of radioactive Cs. The circulation of a lump of contaminated soil in aqueous solution is thus able to separate the fractions that contain high doses of radioactive Cs, which accumulated around the fine soil particles accompanying the clay minerals.[7] The molecular-scale study of Cs adsorption in aqueous solution with a variety of Cs concentrations is required for clay minerals such as saponite. This is of particular importance from the viewpoint of both recycling and reusing soil products contaminated by radioactive Cs in the future, but has escaped attention as a the central research subject so far.

In the geological environment, radioactive Cs released from a nuclear power plant interacts with groundwater in a highly

[a] *Department of Environmental Sciences, Tokyo Gakugei University, Koganei, Tokyo 184-8501, Japan. E-mail: sato-k@u-gakugei.ac.jp*
[b] *Institute of Chemical Technology, University of Stuttgart, 70550 Stuttgart, Germany*

complex manner.[8,9] The radioactivity of ^{137}Cs in groundwater sampled in the area ~35 km north west of the Fukushima Dai-ichi Nuclear Power Plant ranges from 0.0025 to 0.038 Bq L^{-1} in 2011–2013.[10] The concentration of ^{137}Cs in the soil environment has been influenced by a number of environmental factors such as the heavy rains caused by Typhoon Roke and geological conditions.[11] It has been reported from the results of an on-site survey of the Fukushima river system that the radioactivity of ^{134}Cs and ^{137}Cs depends on contamination in the watershed.[12] It is thus of significance to investigate Cs adsorption in aqueous solution as a function of solution concentration to understand the behaviour of Cs in the real environment. In the present study, the adsorption of Cs in aqueous solution across a wide range of Cs^+ concentration levels is studied for a saponite mineral, *i.e.* a silicate clay abundant in the soil environment, by means of a conventional elution test, ^{133}Cs magic-angle-spinning nuclear magnetic resonance (MAS NMR), and the radiocesium interception potential (RIP). The local molecular structures, *i.e.* nanosheet surfaces, nanosheet edges, and oncoming hexagonal cavities, participating in Cs adsorption are qualitatively highlighted based on the results of a recently developed analytical method.[13]

Experimental section

Materials

Synthetic Na-type saponite $Na_{0.66}[Mg_{5.34}Li_{0.66}]Si_8O_{20}[OH]_4$ produced by Kunimine Industries Co. Ltd, Japan, was employed as the Cs-unloaded sample. The Cs loading was conducted by impregnating the Na-type saponite with CsCl aqueous solution, varying the Cs solution concentration from 0 to 2 M. The dehydrated samples were prepared by hearting at 423 K for 24 h under the vacuum condition of ~10^{-5} Torr.

Elution experiment

A Cs elution test was conducted for the Cs-loaded saponite using nitric acid solution of pH = 0. Samples with a mass of 0.2 g were soaked in the nitric acid solution for 2 days. The concentrations of Cs^+ ions eluted into 5 mL of the nitric acid solution were analysed by atomic absorption spectrometry.

^{133}Cs magic-angle-spinning nuclear magnetic resonance

The ^{133}Cs MAS NMR experiments were performed for the hydrated and dehydrated samples using a Bruker Avance III 400WB spectrometer at the resonance frequency of 52.5 MHz. All spectra were recorded at a sample spinning rate of 22 kHz after single pulse excitation with a repetition time of 3 s. The chemical shifts were referenced to a 1.0 M solution of CsCl. The Bruker softwares WINFIT and SOLA of TopSpin3.1 were applied for the deconvolution and simulation of the ^{133}Cs MAS NMR spectra.

Specific Cs adsorption sites

Positronium (Ps) annihilation spectroscopy together with molecular dynamics (MD) simulation of the silicate clays revealed that the local molecular structure was built by the insertion of two nanosheets into the interlayer space in the dehydrated state.[14–16]

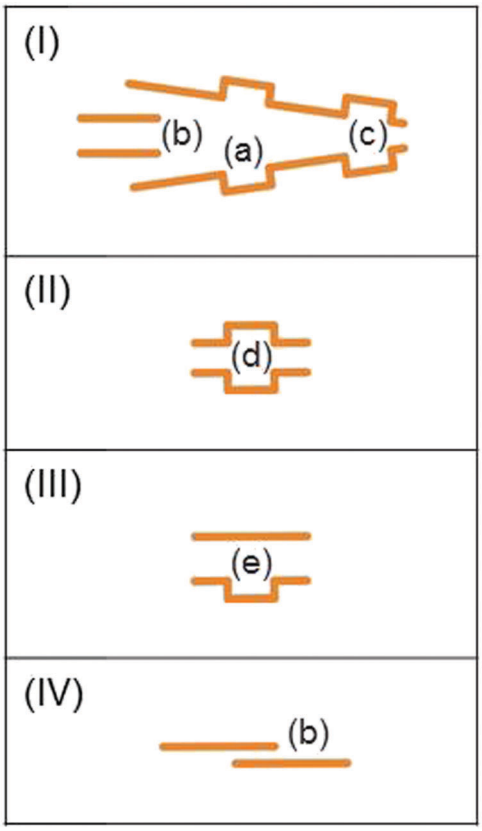

Fig. 1 Schematically illustrated local molecular structures formed by 2D nanosheets in the dehydrated state: (I) two-nanosheet insertion type, (II) oncoming hexagonal cavities, (III) hexagonal cavities, and (IV) steps. Cs adsorption occurs at (a) nanosheet surfaces, (b) nanosheet edges, (c) wedge-shaped parts, (d) nanosheet surfaces in the oncoming hexagonal cavities, and (e) nanosheet surfaces in the hexagonal cavities.

The local structure built by two-nanosheet insertion is schematically shown in Fig. 1 (see (I)). This local molecular structure contains three kinds of Cs adsorption sites: (a) nanosheet surfaces, (b) nanosheet edges, and (c) wedge-shaped parts. Cs ions are physisorbed at the nanosheet surfaces, which are negatively charged because of local compositional and structural fluctuations. Conventional decontamination work generally focuses on this physisorption of Cs ions at the nanosheet surfaces. However, our recent work revealed that heavily adhesive Cs adsorption, so-called specific Cs adsorption, also occurs both at the nanosheet edges and wedge-shaped parts. Surprisingly, Cs adsorbed there cannot be removed by washing with a hydrochloric acid solution of pH = 1.0. ^{133}Cs MAS NMR revealed the existence of Cs_2O (formed by the chemisorption of Cs at the nanosheet edge sites) through an additional broad peak signal at −9 ppm.[17] The chemisorption of Cs with O atoms at the nanosheet edge sites was further identified by FT-IR spectroscopy,[13] where the Si–O vibration band was blue-shifted upon Cs loading. Besides the nanosheet edge sites, the wedge-shaped parts strongly adsorb Cs^+ ions *via* geometrical confinement in addition to physisorption. 2D nanosheets are also able to form other local molecular structures where both sides are hexagonal cavities and one side is a hexagonal cavity (see (II) and (III)).

This journal is © the Owner Societies 2017

In these local molecular structures, Cs physisorption occurs at (d) oncoming hexagonal cavities and (e) hexagonal cavities. The interlayer space shrinks in the dehydrated state, as a result of which the local molecular structure of the oncoming hexagonal cavities becomes geometrically similar to the wedge-shaped part. Furthermore, a step structure can be formed by the 2D nanosheets, which exhibit the nanosheet edge sites (see (IV)). This could act as a chemisorption site, similar to the nanosheet edges in the local structure built by two-nanosheet insertion (I).

Results and discussion

Fig. 2 shows the result of the Cs elution test, where the concentration of Cs^+ ions is plotted as a function of the Cs^+ molarity of the solution. The concentration of Cs^+ ions rapidly increases with increasing Cs^+ molarity up to 0.5 M and gradually increases thereafter, as indicated by arrows. As mentioned above, the Cs chemisorbed at the nanosheet edges or firmly confined within the wedge-shaped parts cannot be removed by washing with a hydrochloric acid solution of pH = 1.0 (see Section 3, Specific Cs adsorption sites). However, the present Cs elution experiment was conducted with a nitric acid solution of pH = 0 (see Section 2.2 of Experimental section). Considering that an acid solution of pH = 1.0 is strong enough to decontaminate the radioactive Cs in the soil environment,[18] the Cs^+ ions eluted by the nitric acid solution of pH = 0 must be those that were physisorbed on the surface of the 2D nanosheets (see the (a), (d), and (e) sites in Fig. 1).

Fig. 3 shows the ^{133}Cs MAS NMR spectra obtained for the dehydrated samples with solution concentrations of 0.5, 0.75, 1, 1.5 and 2 M together with the simulated curves. Qualitatively, similar spectra were obtained for all the samples. As detailed in our previous ^{133}Cs MAS NMR study of a 1 M sample,[17] the dominant signals at around −134 ppm correspond to the Cs^+ interlayer cations physisorbed on the surfaces of the 2D nanosheets (see the (a), (d), and (e) sites in Fig. 1), whereas the additional broad signals at around −15 ppm originate from Cs_2O at the nanosheet edges (see the (b) site in Fig. 1).

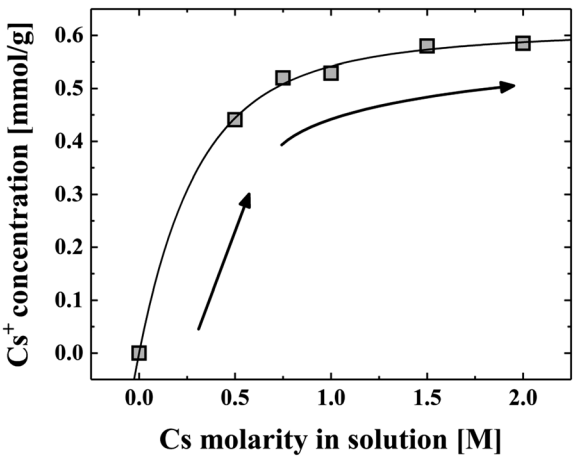

Fig. 2 Concentration of eluted Cs^+ ion as a function of the Cs molarity of the solution. Arrows are drawn for guiding the eyes. The data at 0.5 M was taken from ref. 13.

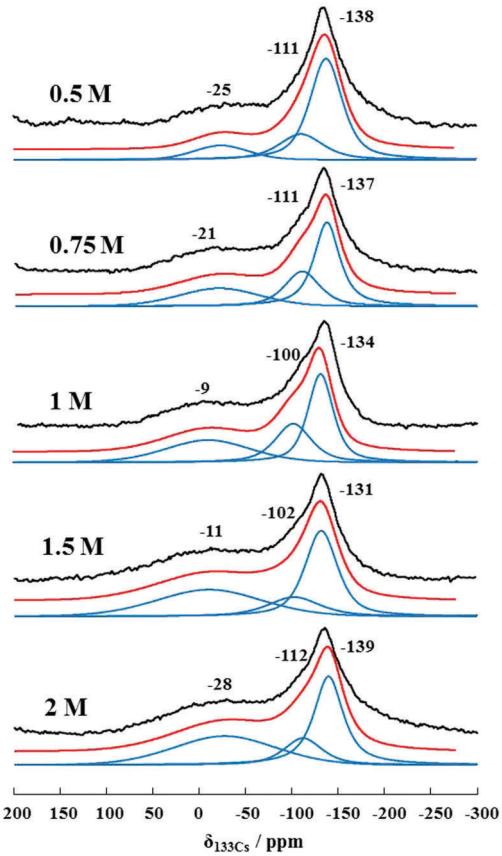

Fig. 3 ^{133}Cs MAS NMR spectra obtained for the dehydrated samples with solution concentrations of 0.5, 0.75, 1, 1.5 and 2 M together with the simulated curves. The data at 0.5 M was taken from ref. 13. The experimental spectra (black) are compared with the simulated ones (red). The blue curves indicate the different signals of the non-equivalent ^{133}Cs species.

Additional shoulders at *ca.* −100 ppm are present at the low-field edge of the dominant signal. They are evidently caused by the wedge-shaped part and oncoming hexagonal cavities at nanosheet surfaces (see (c) and (d) sites in Fig. 1), since these contribute to the additional low-field shoulder at *ca.* −100 ppm in the NMR spectrum, being stronger O coordination sites than the nanosheet surfaces. A similar observation was reported for zeolites, where the strong interactions of Cs cations with O_2 in zeolites X and Y led to a low-field shift of their ^{133}Cs MAS NMR signals.[19]

Here, we outline the analytical procedure for evaluating the concentration of the local molecular structures participating in Cs adsorption, based on the data from ^{133}Cs MAS NMR spectroscopy, RIP, and the elution experiment. Since the Cs adsorption sites (e) of the hexagonal cavities are geometrically the same as those (a) of the nanosheet surfaces, four molecular sites (a), (b), (c), and (d) can be considered in the following calculations. For the 0.5 M sample as an example, the simulated result of the ^{133}Cs MAS NMR study gives the relation among the concentrations of molecular sites: (a) nanosheet surfaces, c_s, (b) nanosheet edges, c_e, (c) wedge-shaped parts, c_w, and (d) oncoming hexagonal cavities, c_o. The relation is as follows:

$$c_s : c_e : (c_w + c_o) = 0.65 : 0.13 : 0.22 \quad (1)$$

yielding the following three equations:

$$\begin{cases} c_s = \dfrac{65}{13} c_e \\ c_s = \dfrac{65}{22}(c_w + c_o) \\ c_e = \dfrac{13}{22}(c_w + c_o) \end{cases} . \quad (2)$$

These equations are unfortunately in an indeterminate form, with four parameters, thus requiring additional equations to obtain the solution. These are provided by the results of the elution experiment and RIP. Upon hydration, the interlayer space expands and the population of Cs confined in the oncoming hexagonal cavities is released to be hydrates. The result of the elution experiment thus provides the relation between c_s and c_o as,

$$c_s + c_o = 441, \quad (3)$$

reasonably assuming that one Cs^+ cation is infilled per hexagonal cavity of the nanosheet surfaces. Employing $c_w = 9 \times 10^{-2}$ mmol kg^{-1} obtained from the results of RIP, the values of c_s, c_e, and c_o can be calculated to be 330, 66, and 111 mmol kg^{-1}, respectively.

The concentrations of three molecular sites, *i.e.* nanosheet surfaces, c_s, nanosheet edges, c_e, and oncoming hexagonal cavities, c_o, obtained in the same manner for the samples with the different solution concentrations are shown in Fig. 4. Here, we assume that the concentration of wedge-shaped parts is consistently the same for all the Cs-loaded samples, because Cs adsorption at the wedge-shaped parts is easily saturated at a solution concentration of $\sim 10^{-3}$ M.[20] It is seen that the concentrations of the three molecular sites all increase with increasing Cs^+ molarity of the solution. This indicates that more Cs^+ ions adsorb at the nanosheet surfaces, nanosheet edges, and oncoming hexagonal cavities in more highly concentrated Cs solutions. Consistently with the concentration of Cs^+ ions obtained by the elution test (see Fig. 1), the c_s value rapidly increases with increasing solution concentration up to 0.5 M and then gradually increases up to 2 M. The similarity of the solution-concentration dependences could be a result from the fact that both are determined by Cs physisorption at the nanosheet surfaces, which is saturated at the lower solution concentration.

In contrast, the concentration of oncoming hexagonal cavities, c_o, increases with the Cs^+ molarity of the solution more slowly than that of nanosheet surfaces, c_s, indicating that adsorption of Cs into the oncoming hexagonal cavities is less favourable than that on the nanosheet surfaces. The concentration of the nanosheet edges c_e continues to slowly increase with the Cs^+ molarity of the solution up to 2 M, indicating that the adsorption of Cs there is the most difficult among the three adsorption sites. The distinct adsorption properties of the three molecular sites presumably arise from the local geometrical environments, though Cs^+ ions equally enter into the adsorption process. The oncoming hexagonal cavities are geometrically restricted compared with the nanosheet surfaces.

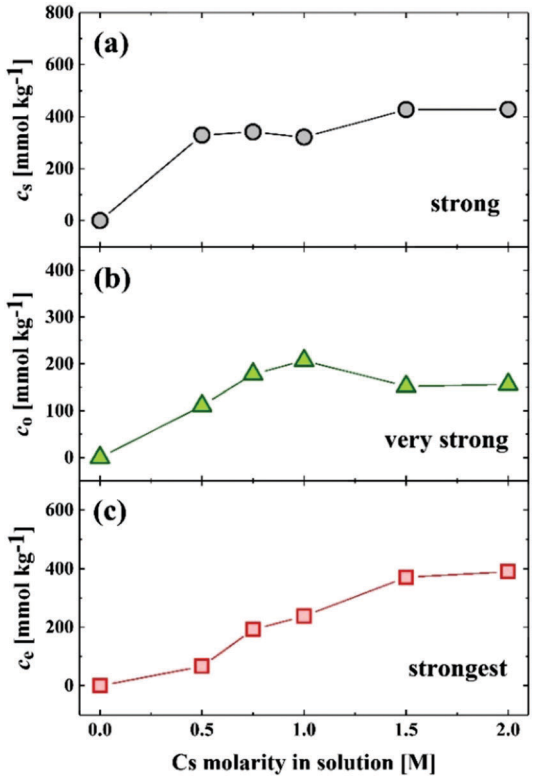

Fig. 4 Concentrations of nanosheet surfaces, c_s (gray circles), oncoming hexagonal cavities, c_o (green triangles), and nanosheet edges, c_e (red squares), as a function of the Cs molarity of the solution. The data at 0.5 M was taken from ref. 13. The adhesivities at the nanosheet surfaces, oncoming hexagonal cavities, and nanosheet edges are described in the (a), (b), and (c), respectively. The wedge-shaped parts have the adhesivity of "very strong".

The adsorption of Cs into the oncoming hexagonal cavities is thus less probable than that on the nanosheet surfaces. Since the chemisorption of Cs occurs at the nanosheet edges in contrast with other physisorption sites such as nanosheet surfaces, the adsorption of Cs at the nanosheet edges is the most difficult among the three molecular sites. Considering the reported radioactivity of ^{137}Cs in groundwater and river systems,[10] the adsorption of Cs at the nanosheet surfaces, nanosheet edges, and oncoming hexagonal cavities identified in the present work is far from saturation (see Fig. 4). This suggests that the three above-mentioned molecular sites are responsible for the adsorption of Cs in the real soil environment of the Fukushima area.

One may consider why such a large amount of nanosheet edges were found to participate in Cs adsorption in the present study. We expect that besides the local structure (I) depicted in Fig. 1, other local molecular structures capable of forming nanosheet edges are also available. One such molecular structure could be the steps that result from the stacking of 2D nanosheets (see (IV) in Fig. 1). The step structure is easily formed because of its enhanced stability in the agglomeration of 2D nanosheets. In addition to the steps, there may also be kink structures contributing to the formation of such a high concentration of nanosheet edges.

 This journal is © the Owner Societies 2017

As mentioned in the introduction, the process of volume reduction for contaminated soil scraped from the soil surface involves water treatment to eliminate the high-dose fractions, which contain smaller particles. This is based on the premise that the radioactive Cs ions are physisorbed on the nanosheet surfaces of the clay minerals. It should be noted here, however, that the concentrations of the three molecular sites participating in Cs adsorption are all approximately similar, with differences of roughly a few hundred mmol kg^{-1} among them. Specifically, the concentration of nanosheet edge sites amounts to ~13% at the solution concentration of 0.5 M. The percentage increases to ~27%, ~31%, ~39%, and ~40% at 0.75, 1, 1.5, and 2 M, respectively. In view of the decontamination of radioactive Cs from clay minerals, the nanosheet edge sites are of particular significance because of their capability for heavily adhesive Cs adsorption. The present results strongly imply that the nanosheet edges should be targeted as the local molecular sites for the future decontamination of radioactive Cs, in addition to the nanosheet surfaces.

The local molecular structure built by the insertion of two nanosheets into the interlayer space, as discussed above, predominantly exists in the dehydrated state. According to our recent rheological model of 2D nanosheet agglomeration,[14] one of the two nanosheets is gradually released with increasing hydration, as a result of which a local molecular structure built by the insertion of one nanosheet eventually becomes dominant in the hydrated state. The summation of the numbers of the one- and two-nanosheet insertion types is preserved regardless of the hydration degree, the concentration of the wedge-shaped parts thus being entirely unchanged over the whole range of hydration degrees.

Upon hydration, the interlayer spaces expand and a large amount of H_2O molecules physisorb onto the Cs^+ cations there. Some of the Cs^+ cations form Cs hydrates in the interlayer spaces while others remain at the surfaces, as predicted by MD simulations.[21] The Cs^+ cations that escape from forming hydrates can adsorb at the nanosheet edge sites and wedged-shaped parts. The small fraction of nanosheets released from the two-nanosheet insertion structure are deposited to form step structures, but this does not strongly influence the total amount of nanosheet edge sites participating in Cs adsorption at any degree of hydration. In contrast, the concentrations of nanosheet surfaces and oncoming hexagonal cavities participating in Cs adsorption vary as a function of hydration. It is emphasized that the qualitative description of the local molecular sites of nanosheet edges and wedge-shaped parts remains unchanged regardless of the hydration degree.

Conclusions

To aid the ongoing decontamination work of radioactive ^{137}Cs from soil, the adsorption properties of Cs in aqueous solution across a wide Cs^+ concentration range were investigated for a saponite clay mineral by means of a conventional elution test, MAS NMR spectroscopy, and RIP. Based on a recently developed analytical method, the concentrations of nanosheet surfaces, nanosheet edges, and oncoming hexagonal cavities participating in Cs adsorption were successfully determined to be a few hundred mmol kg^{-1}. The nanosheet surfaces, nanosheet edges, and oncoming hexagonal cavities identified in the present work represent possible the Cs adsorption sites in the real geological environment. The concentrations of all three molecular sites increase with increasing Cs concentration in aqueous solution, indicating that a higher population of Cs^+ ions can be adsorbed there in more concentrated Cs solutions. The concentration of oncoming hexagonal cavities participating in Cs adsorption increases with the Cs^+ molarity of the aqueous solution more slowly than that of nanosheet surfaces, indicating that Cs adsorption into the oncoming hexagonal cavities is more difficult than that onto the nanosheet surfaces. The concentration of nanosheet edges increases more slowly with increasing Cs^+ molarity of the aqueous solution, because Cs chemisorption occurs there. The population of Cs at the nanosheet edges participating in heavily adhesive Cs adsorption was found to be 13–40% and these sites should be targeted for decontamination in the future.

Acknowledgements

The authors are indebted to K. Fujimoto (Tokyo Gakugei University), K. Kawamura (Tokyo Institute of Technology), N. Shikazono (Keio Univeristy, deceased), S. Nakashima (Kyusyu Environmental Evaluation Association), K. Ito (National Institute of Advanced Industrial Science and Technology), and M. Kamaya (Kogakuin University) for fruitful discussions. One of the authors (K. S.) would like to thank Alexander von Humboldt Foundation (AvH), Fachbereich Physik der Universitaet Stuttgart, and Max-Planck-Institut fuer Festkoerperforschung for their financial supports. This work was partially supported by a Grant-in-Aid of the Japanese Ministry of Education, Science, Sports and Culture (Grant No. 16K05394).

References

1 Web Site of Ministry of the Environment, Government of Japan, Outline of the Implementation of the Act on Special Measures, available at: http://josen.env.go.jp/en/framework/.
2 Web Site of Ministry of the Environment, Government of Japan, Progress in the Special Decontamination Area (as of April1, 2017), available at: http://josen.env.go.jp/en/decontamination/.
3 Web Site of Ministry of the Environment, Government of Japan, Decontamination Guidelines, available at: http://josen.env.go.jp/en/framework/.
4 Web Site of Ministry of the Environment, Government of Japan, Aspect for 5 year *ad hoc* Policy on Interim Storage Facility (1), available at: http://josen.env.go.jp/en/storage/.
5 T. Yasutaka, W. Naito and J. Nakanishi, *PLoS One*, 2013, **8**(1), e75308.
6 for example, K. Yukumatsu, N. Nomura, F. Mishima, Y. Akiyama and S. Nishijima, *Prog. Supercond. Cryog.*, 2016, **18**, 10.
7 K. Ishii, A. Terakawa, S. Matsuyama, Y. Kikuchi, F. Fujishiro, A. Ishizaki, N. Osada, H. Arai, H. Sugai, H. Takahashi,

K. Nagakubo, T. Sakurada, H. Yamazaki and S. Kim, *Nucl. Instrum. Methods Phys. Res., Sect. B*, 2014, **318**, 70.
8 K. Fujimoto, K. Sato and M. Nakata, *J. Phys. Soc. Jpn.*, 2017, **86**, 034901.
9 K. Sato, K. Fujimoto, M. Nakata and N. Shikazono, *J. Phys. Soc. Jpn.*, 2013, **82**, 014901.
10 S. Iwagami, M. Tsujimura, Y. Onda, M. Nishino, R. Konuma, Y. Abe, M. Hada, I. Pun, A. Sakaguchi, H. Kondo, M. Yamamoto, Y. Miyata and Y. Igarashi, *J. Environ. Radioact.*, 2017, **166**, 458.
11 S. Nagao, M. Kanamori, S. Ochiai, S. Tomihara, K. Fukushi and M. Yamamoto, *Biogeosciences*, 2013, **10**, 6215.
12 S. Nagao, M. Kanamori, S. Ochiai, K. Suzuki and M. Yamamoto, *Prog. Nucl. Sci. Technol.*, 2014, **4**, 9.
13 K. Sato, K. Fujimoto, W. Dai and M. Hunger, *J. Phys. Chem. C*, 2016, **120**, 1270.
14 K. Sato, K. Fujimoto, K. Kawamura, W. Dai and M. Hunger, *J. Phys. Chem. C*, 2012, **116**, 22954.
15 K. Sato, K. Numata, W. Dai and M. Hunger, *Phys. Chem. Chem. Phys.*, 2014, **16**, 10959.
16 K. Sato, K. Numata, W. Dai and M. Hunger, *Appl. Phys. Lett.*, 2014, **104**, 131901.
17 K. Sato, K. Fujimoto, W. Dai and M. Hunger, *J. Phys. Chem. C*, 2013, **117**, 14075.
18 Y. Wen, J. Song, W. Liu and Z. Qin, *J. Radioanal. Nucl. Chem.*, 2002, **253**, 167.
19 H. Liu and C. P. Grey, *Microporous Mesoporous Mater.*, 2002, **53**, 109.
20 A. Cremers, A. Elsen, P. De Preter and A. Maes, *Nature*, 1988, **335**, 247.
21 M. Nakano, K. Kawamura and Y. Ichikawa, *Appl. Clay Sci.*, 2003, **23**, 15.

 This journal is © the Owner Societies 2017